Monatshefte für Chemie 129, 535–544 (1998)

Monatshefte für Chemie
Chemical Monthly

Solution Structure of Mesobiliverdin XIIIα Bridged Between the Propionic Acid Substituents [1]

Joaquim Crusats, Pilar Benitez, Joan-Anton Farrera, Raimon Rubires, and **Josep M. Ribó***

Departament de Química Orgànica, Universitat de Barcelona, E-08028 Barcelona, Spain

Summary. The solution structure of two intramolecular diesters (methylene and 1,3-propylidene) of mesobiliverdin-XIIIα was studied and compared with that of the corresponding dimethyl ester. The UV/Vis absorption spectra, chiral discrimination with ethyl (*S*)-(−)-lactate, and the ^{1}H NMR spectra (ROESY) show that the cyclization of the propionate substituents of biliverdins does not significantly affect the helix structure or its (*P*) ⇌ (*M*) interconversion. The internal methylene diester does not show conformational heterogeneity of the propionate substituents and probably exists only in one diastereomeric form. In this case, the results point to a simultaneous racemization of the tetrapyrrole helix and the bridge cycle. The methylene diester of mesoprotoporphyrin was also synthesized. In this case, the geometry of the propionate chains is probably similar to that present in some hemoproteins.

Keywords. Bile pigments; Induced circular dichroism.

Zur Struktur des über die Propionsäurereste überbrückten Mesobiliverdins XIIIα in Lösung

Zusammenfassung. Die Struktur zweier zyklischer Ester (Methylendioxy- und 1,3-Dipropylenoxy-) des Mesobiliverdin XIIIα in Lösung wurde untersucht und mit der des entsprechenden Dimethylesters verglichen. Die UV/Vis-Spektren, die chirale Diskriminierung mit Äthyl-(*S*)-(−)-Laktat und die ^{1}H-NMR-Spektren (ROESY) zeigen, daß durch interne Zyklisierung über die Propionsäure die Helixstruktur oder die (*P*) = (*M*) Konvertierung kaum beinflußt wird. Beim zyklischen Methylendioxyester weisen die Propionsäuresubstituenten verschiedene Konformationen auf. Wahrscheinlich existiert nur eine einzige diastereoisomere Form unter gleichzeitiger Racemisierung der Tetrapyrrolhelix und des Ringes der Brückenester. Der Methylendioxyester des Mesoprotoporphyrins wurde ebenfalls dargestellt. Die Geometrie seiner Propionatreste entspricht wahrscheinlich derjenigen, die in einigen Hämoproteinen gefunden wurde.

Introduction

For the biliverdins of the natural series [2] it is possible to obtain a bridge between the propionic acid chains by formation of the diester of a short-chain α,ω-

* Corresponding author

alkanediol [3]. Recently it has been shown that the same cyclization process can also be performed in the case of porphyrins [4].

In the anchoring of bilatrienes and porphyrins in proteins (biliproteins and hemoproteins) and in the complexation of bilirubin by serum albumin, the ionic interaction of the carboxylate groups of the propionic substituents with basic groups of the protein possibly play an important role. The internally cyclized tetrapyrrolic pigments mentioned above are good models for the investigation of the role of the propionate substituents under the boundary conditions of the structural constrictions imposed upon the prosthetic groups of bili- and hemoproteins. In fact, the distance between the two carboxylic groups in these internal diesters is of the same order of magnitude as in hemoproteins [5].

Here we present results on the structure and association in the solution of two intramolecular diesters of mesobiliverdin XIIIα (**5**, **6**; see Scheme) and the methylene diester of mesoporphyrin IX (**7**). The results are compared with those obtained for their open chain dimethyl esters.

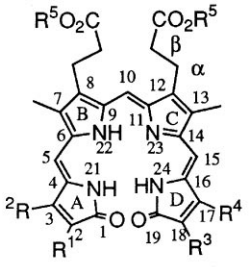

1: $R^1 = R^4 = R^5 =$ Me; $R^2 = R^3 =$ Et
2: $R^1 = R^4 =$ Me; $R^5 =$ H; $R^2 = R^3 =$ Et
3: $R^1 = R^3 = R^5 =$ Me; $R^2 = R^4 =$ Et
4: $R^1 = R^3 =$ Me; $R^5 =$ H; $R^2 = R^4 =$ Et

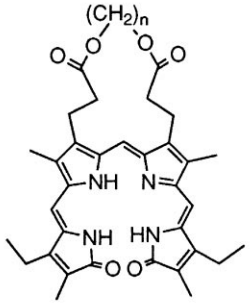

5: $n = 1$
6: $n = 3$

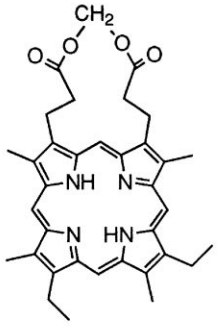

7

Results and Discussion

The cyclic esters of mesobiliverdin XIIIα (**5**, **6**) and of mesoporphyrin IX (**7**) (see Scheme) were obtained by reaction of the dicaesium salt of the tetrapyrrole pigments with diiodomethane (for the C1 diesters) or with 1,3-diiodopropane (for the C3 diesters) in *DMSO* at high dilution [3].

For a broad range of concentrations, all reported biliverdins show a behaviour consistent with *Lambert-Beer*'s law. Vapor osmometry measurements confirm a very low degree of association (see Experimental) for the cylclic as well as for the open-chain diesters. This is consistent with the reported behaviour of 1,19-bilindiones which associate in solution when free carboxylic acid groups are present [6, 7] and means that bilindiones do not show the same behaviour as porphyrins where a strong association occurs because of the interaction between the π systems [8]. Probably, for bilindiones their non-planar helical structure and the strong polarization exerted by the lactam carbonyl groups do not permit a suitable geometry for the hydrophobic interactions which are present in the case of porphyrins.

UV/Vis absorption and luminescence spectra

The absorption spectra of **5** and **6** in several solvents do not differ significantly from those of the corresponding dimethyl ester (**3**) (see Table 1).

The 1,19-bilindiones show absorption spectra in the visible range with two important bands whose intensity ratio can be taken as an indication of the bilatriene conformation [9]; the most stable geometry of 1,19-bilindiones corresponds to a helicoidal *Z,Z,Z,syn,syn,syn* structure with intensity ratios between the high- and the low-energy absorption of about 3:1. More stretched structures show an increase in the relative intensity of the low-energy band. In this respect, the UV/Vis spectra of **3**, **4**, **5**, and **6** (Table 1 and Fig. 1) point to a similar structure of the bridged and the open esters. However, the small difference in the position of the lowest-energy absorption (630 nm for free acid, dicarboxylate, and dimethyl ester compared to 620 nm for the cyclic esters) point to a less planar structure of the cyclic esters.

For **5** and **6** as well as for **3** we could not detect luminescence spectra. Biliverdins show a very efficient deexcitation process as a consequence of proton exchange between tautomeric centres and, maybe, through the rotational movement around the exocyclic single bonds [10]. The absence of luminiscence for the

Table 1. UV/Vis absorption and CD data in ethyl (*S*)-(−)-lactate of bilin-1,19-diones **3–6**

	UV/Vis[a]		CD	
	λ_{max} (nm)	ε ($mol^{-1} \cdot 1 \cdot cm^{-1}$)	λ_{max} (nm)	$\Delta\varepsilon$ ($mol^{-1} \cdot 1 \cdot cm^{-1}$)
3	366	46000	360	+11.7
	630	13000	666	−7.0
4[b]	370	46500	360	+8.9
	630	13700	660	−4.4
5	366	47000	360	+10.1
	620	14000	660	−5.1
6	366	43000	360	+8.9
	620	13000	660	−5.3

[a] $3.5\ 10^{-5}\ mol \cdot l^{-1}$ solutions; λ_{max} and ε values do not differ significantly from the data obtained in CH_2Cl_2; [b] diammonium salt of **4**, obtained by bubbling a small amount of ammonia through the solution; ε values are approximate

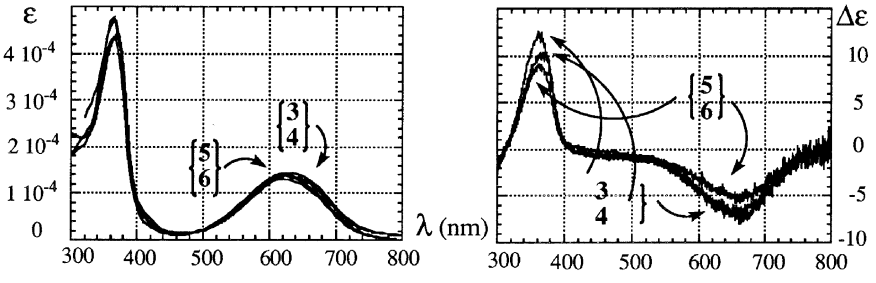

Fig. 1. Visible absorption spectra and induced circular dichroism in ethyl (*S*)-(−)-lactate of mesobiliverdins (see Table 1)

cyclic esters of biliverdins confirms the low contribution of the deactivation pathways of the rotation processes at C10 *e.g.* through structures of type *Z*,*Z*,*Z*,*syn*,*anti*,*syn*.

Solvent induced circular dichroism

The most stable structure of bilin-1,19-diones in solution (*Z*,*Z*,*Z*,*syn*,*syn*,*syn*) is that of a helix, *i.e.* an inherently dissymmetric chromophore. The (*P*)⇌(*M*) interconversion barrier is low [11]. This does not allow the isolation of the enantiomers at room temperature conditions, but chiral discrimination can be easily induced by a homochiral solvent [12] or through the diasteromeric interactions of the helices with chiral elements covalently bound to the bilatriene [13]. Solutions of **3** in presence of ethyl (*S*)-(−)-lactate show, as expected, induced circular dichroism (CD) similar to that described for other open chain biliverdin esters [11a]. Under the same experimental conditions, **7** does not show any induced CD signal. **5** and **6** show similar $\Delta\varepsilon$ values; they do not differ significantly from that detected for **3** and the diammonium salt of **4** (Table 1 and Fig. 1). This corresponds, within experimental error, to the similar chiral discriminations of **3**, **5**, and **6** (assuming similar rotational strength for the three compounds and for their heteroassociates with the homochiral ethyl lactate). The chiral discrimination corresponds to the presence of a chiral excess of a helix derived from the *Z*,*Z*,*Z*,*syn*,*syn*,*syn* structure, which is consistent with previous results reporting chiral discriminations on C2,C18-bridged biliverdins, *e.g.* in the case of the biliverdin IXα dimethyl ester (**1**) [13j].

The chiral discrimination observed with ethyl (*S*)-(−)-lactate corresponds to an excess of the (*P*) helix, affording a negative CD value for the absorption at low energy (650 nm) and a positive value for the absorption at 370 nm.

For a discussion of the chiroptical properties of bilindiones see pp 423–430 of Ref. [2b]. The sign of the CD corresponding to the two visible region absorption bands allows to infer the absolute configuration of the helix [14] using the dipole velocity approximation for a simple model [14a], for semiempiric-CI [14b], and for PPP-CI [14c] calculations. Our results obtained by *ab initio* [14d] calculations agree with these previous results.

The previously described difference between λ_{max} of the low-energy transition of the UV/Vis absorption and the CD peak ($\approx$30 nm) for the acyclic esters can also be detected for the cyclic esters. This difference can be attributed to a conformational heterogeneity of the bilindione as well as to the formation of heteroassociates with the solvent. Some years ago, this difference has been attributed to the presence of stretched structures of very different geometry (much more extended) than those corresponding to the *Z*,*Z*,*Z*,*syn*,*syn*,*syn* structure [12a]. However, because of the accumulated knowledge on the structure of bilindiones, this conformational heterogeneity has to be attributed to the formation of heteroassociates of the helix structure with the homochiral solvent and to small changes of the torsion angles at the exocyclic single bonds [15].

In conclusion, the results discussed above suggest that the energetic relations in the helicoidal structure of biliverdins are not significantly modified by intramolecular cyclization of the propionate groups.

^{1}H NMR spectra

The ^{1}H NMR spectra of the cyclic esters **5** and **6** are similar to that of the dimethyl ester **3**; olefinic, methyl, and ethyl protons of the biliverdin skeleton display similar chemical shifts. The most significant difference between these spectra, in addition to the protons of the ester groups, arises from the CH_2-CH_2COO*R* spin system (Table 2 and Fig. 2). For **6** and the open-chain diesters of biliverdins (*e.g.* **1** and **3**), an A_2X_2 (A_2M_2) system is observed, *i.e.* two triplets with J_{AX} about 8 Hz. However, for **5**, an AA′XX′ system is formed (see Fig. 2); compared to **3** and **6**, the chemical shift of the CH_2 group bound to the ring appears at lower field (0.04 ppm), and the signal of the CH_2 bound to the carbonyl carbon atom appears at higher field (0.02 ppm). This AA′XX′ spin system can only be simulated assuming coupling constants with different values, for instance $J_{AA'} \approx J_{XX'} = 17$–$14$ Hz, $J_{AX} = 8$–10 Hz, and $J_{AX'} = 2$–3 Hz (see Fig. 2).

These results suggest that the conformational heterogeneity of the propionate chains of **6** in solution is comparable to that of the open-chain diesters and that **5** shows only one stable conformation for the bridge cycle. In NMR, symmetrically substituted 1,19-bilindiones, owing to the N-H tautomerism between N_{22} and N_{23}, have C_2 symmetry. The formation of a bridge between the propionate groups could lead to a new element of chirality; in the case of only two conformations of the bridge cycle, we would have the stereoisomers (*P*,*P*), (*M*,*M*), (*P*,*M*), and (*M*,*P*). The A_2X_2 (A_2M_2) systems of **6** and **3** with $J_{AX} \approx 8$ Hz point to the presence of several conformations of the propionate chains and fast racemization of the tetrapyrrolic helix. For **5**, the clear difference in the values of the coupling constants J_{AX} and $J_{A'X}$ suggests that this diastereomeric heterogeneity does not exist. For the

Table 2. ^{1}H NMR spin systems and chemical shifts ($CDCl_3$, δ in ppm) of the propionate groups of biliverdins

	–C*H*$_2$–CH$_2$–CO–	–CH$_2$–*CH*$_2$–CO–	Spin System
1	2.93	2.55	A_2X_2
3	2.93	2.55	A_2X_2
5	2.97	2.52	AA′XX′
6	2.94	2.54	A_2X_2

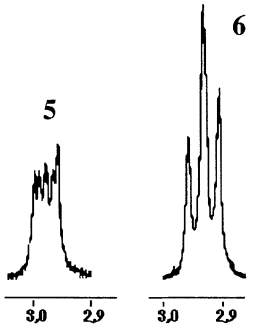

Fig. 2. Part A of the spin system of the –CH_2–CH_2–CO– substituents

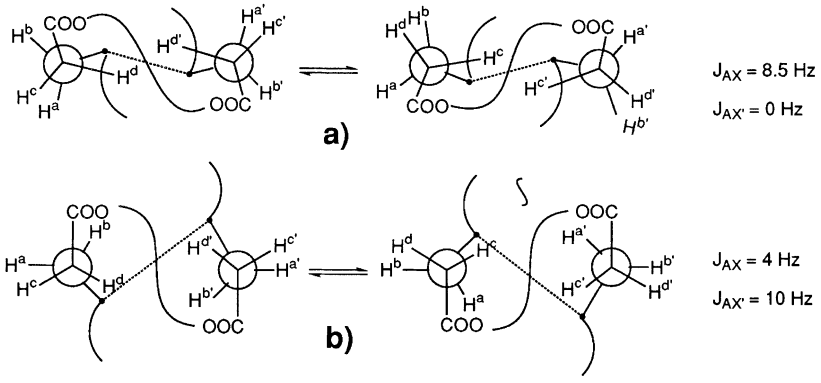

Fig. 3. Models *a*) and *b*) (see text) and estimated *J* values of the AA′XX′ spin system; A = H^a and $H^{a'}$, A′ = H^b and $H^{b'}$, X = H^c and $H^{c'}$, X′ = H^d and $H^{d'}$

propionate chains in the case of fast tautomerization (N_{22}–N_{23}), fixed conformation, and absence of interconvension between esteroisomers, an ABXY system should be expected for each pair of enantiomers. The detection of only one AA′XX′ system, or of an apparent A_2X_2 (A_2M_2) system, implies a fast racemization, *i.e.* tautomerization, helix interconversion, and conformational interconversion of the bridge cycle. According to the accepted values of ^3J and ^2J for aliphatic chains and using the same approach as used for the conformational analysis of cyclic hydrocarbons and carbohydrates [16], the experimental AA′XX′ system of **5** can be explained by one of the following conformations (see Fig. 3):

a) open *synclinal* conformations (dihedral angle C-Cα-Cβ-C of 90–100°);

b) closed *antiperiplanar* conformations (dihedral angle C-Cα-Cβ-C of 140–150°).

Antiperiplanar (180°) and "open" *antiperiplanar* conformations can be excluded owing to the torsional stress imposed upon the bridge cycle. Combinations corresponding to one propionate oriented *synclinal* and the other *antiperiplanar* result in similar J_{AX} and $J_{AX'}$ values (apparent A_2X_2 spin system); 60° *synclinal* conformations would result in low and only slightly differing *J* values ($\approx$2 and 6 Hz). Open force field calculations [17] show that models *a*) and *b*) correspond to the most stable conformations of **5**. Model *b*) is about 4.2 kJ · mol^{-1} less stable than model *a*). This small energy difference does not rule out model *b*). However, model *b*) can be rejected taking into account the NOEs detected in the ROESY experiments and the geometry of the models (see Table 3).

For all biliverdins reported here, the olefinic protons at C5 and C15 show NOEs with the alkyl protons at C3, C7, C13, and C17, and the olefinic proton at C10 with the methylene groups of the propionate substituents. This, supported by the absence of NOEs between the olefinic protons and H-N, is a proof of the *Z*,*Z*,*Z*,*syn*,*syn*,*syn* structure [18]. However, differences are observed in the relative intensities of the NOEs between the olefinic proton at C10 and the methylene groups of the propionate substituents (see Table 2).

Table 3. Relative intensities of the ^{1}H NMR NOEs (ROESY, 500 MHz) at 450 ms spin-lock time

	Detected NOE				
	a	b	c	d	e
3	++	++	+	++	+
5	++	++	+	++	+
6	++	++	+	++	++
7				++	+

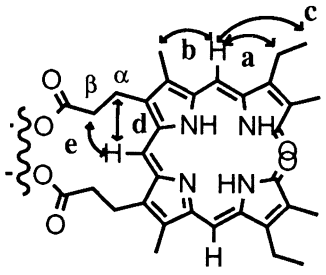

We have studied the dependence of the intensity on the spin-lock time (ROESY) for several bile pigments. The signal decays are very different, and most of the NOEs correspond to more than two spin systems. This prohibits the application of quantitative relationships. As a consequence, the results are interpreted in a semiquantitative mode in the sense of Ref. [19].

For the open chain diesters, the NOE corresponding to β-CH_2 is less intense than that for the α-CH_2; this agrees with the relative distances of these methylene groups to the proton at C10. However, for **6** these two NOEs are of similar intensity. The geometries of **5** obtained by open force field calculations show that in the case of model *b*) the distance between the H-C10 and the protons at β-CH_2 is shorter than for α-CH_2 (4.1 Å compared to 3.1 Å for the internal H atom of the α-CH_2 and the β-CH_2), *i.e.* model *b*) should show NOEs with relative intensities of inverse order to the experimental values. However, model *a*) (see Fig. 4), in addition to being the most stable conformation in the open force field calculations, gives relative distances of the CH_2 groups in agreement with the relative order of the experimental NOEs (4 Å compared to 5 Å for the internal H atom of the α-CH_2 and the β-CH_2, respectively. Figure 4 shows the structure corresponding to model *a*). In the case of **6** the same calculations result in several stable conformations of similar energy with similar distances between the α and the β methylene groups, which agrees with the experimental relative NOEs and the conformational heterogeneity detected.

The interpretation of the ^{1}H NMR (500 MHz) spectra of **7** is rather difficult because of the formation of homoassociates. The previously reported high field ^{1}H

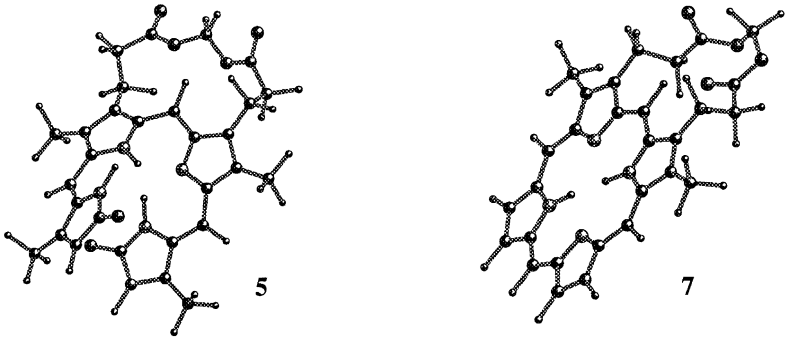

Fig. 4. Molecular models of the most stable structures of **5** and **7** calculated by open force field methods (see text)

NMR spectra of mesoporphyrin IX dialkyl esters [20] show that they correspond to low symmetry species and are concentration dependent, probably because of the formation of dimers. Upon changing the concentration, in addition to changes in the chemical shifts of the olefinic, methyl, and ethyl proton, porphyrin **7** shows important changes of the spin system of the propionate chains. The interpretation of these spin systems is rather difficult because of the unsymmetrical substitution of the porphyrin ring. However, the presence of one or several AA′XX′ systems can be excluded. Probably, we have to deal with a combination of ABXY or an apparent A_2XY system. The question remains open whether this could be attributed to the formation of homoassociates or to the increase in the interconversion barrier of the bridge cycle.

Open force field calculations show that in the more stable conformation the bridge cycle has *cisoid* propionate chains (dihedral angle around C-Cα-Cβ-C of contrary sign for both propionate chains). In this respect, the propionate chains of the biliverdin chain are *transoid* (dihedral angle around C-Cα-Cβ-C of equal sign for both propionate chains). The planarity of the porphyrin ring, compared to the non planar biliverdin, would determine this conformation. This *cisoid* conformation of the propionate chains of the porphyrin can be detected in hemoproteins where the propionate groups are ionized by direct interaction with basic amino acid residues (*e.g.* catalases) [5, 21].

Application of the force field methods used in the case of Fig. 4 result – for the case that both carboxylate groups are hydrogen bound to a water molecule – in a structure very similar to that detected in catalases by X-ray analysis [5, 21]. The most significant difference with respect to the structure of Fig. 4 is the position of the water molecule with respect to the methylene group. The water molecule is located below the position of the methylene group because of the smaller angle of H–O–H compared to O–CH_2–O.

For other hemoproteins, *e.g.* in myoglobins, where the water ionized porphyrin carboxylates do not form ionic bonds with the protein skeleton, the propionate chains are *anti*, *i.e.* in a conformation similar to that expected in the case of the open chain diesters.

Experimental

UV/Vis spectra were recorded using a Perkin-Elmer Lambda 5 spectrometer. Luminescence spectra were recorded with an Aminco-Bowman Series 2 instrument with a Xe lamp (1.5 W). Circular dichroism measurements were performed on a Jason J720 instrument using cuvettes of 1 cm thickness and $3 \cdot 10^{-5}$ mol $\cdot$ l^{-1} solutions in ethyl (*S*)-(−)-lactate previously filtered through potasium carbonate. Vapour osmometry measurements were performed with a Knauer 0587 instrument in $CHCl_3$ at 40°C.

Calculations were performed on a SG MIPS R8000 computer. For force field calculations, the Universal Force Field with Charge Equilibration scheme [18] was used on the interface Cerius 2 (Molecular Simulations). For *ab inito* and CIS calculations, Gaussian 94 [14d] was used on the Cerius 2 interface (3–21G and 6–31G* basis set; detailed results will be published elsewhere).

^{1}H NMR and ROESY spectra were recorded with varian Unity 300 (300 MHz) and a Varian Unity 500 (500 MHz) spectrometers using $CDCl_3$ (previously filtered through basic alumina I) as solvent and *TMS* as internal reference. The ROESY experiments were carried out at spin lock times of 50, 100, 150, and 450 ms. However, the relative intensities between the signals used for the *semi*-quantitative evaluation (Table 3) were evaluated only from the experiments at 450 ms.

The preparation of mesobiliverdin IXα (**2**) [22], its dimethyl ester (**1**) [22], mesobiliverdin XIIIα (**4**) [23], and its dimethyl ester (**3**) [23] from bilirubin IXα (Janssen Chimica) have been described in the literature. Mesobiliverdin XIIIα methylene diester (**5**) [3], mesobiliverdin XIIIα propane-1,3-diyl diester (**6**) [3], and mesoprotoporphyrin IX methylene diester (**7**) [4] were obtained as previously described. Physical and chemical data of these substances have already been reported [3, 4]. Other data not yet published are described in the text (ROESY, CD, UV/Vis; Tables 1–3, Fig. 1–2).

Fluorescence spectra for **3**, **5**, and **6** ($1 \cdot 10^{-5}$ mol $\cdot$ l^{-1} solutions in CH_2Cl_2, 1 cm cuvette, detector at 650 V) could not be detected.

Vapour osmometry measurements in $CHCl_3$ in the concentration range of $3 \cdot 10^{-3}$–$3 \cdot 10^{-2}$ molal show osmotic coefficients ($\Phi = M/M_{exp}$) for **3**, **5**, and **6** of 0.96±0.02 without detectable influence of the concentration.

Acknowledgments

We gratefully acknowledge support by DGICYT (PB93-1257) and the *Generalitat de Catalunya* (SGR96-00098).

References

[1] A large part of the work corresponds to the PhD Thesis of Crusats J (1996) University of Barcelona

[2] a) IUPAC-IUB, Nomenclature of tetrapyrroles (1987) Pure Apple Chem **59**: 779; b) Falk H (1989) The Chemistry of Linear Oligopyrroles and Bile Pigments. Springer, Wien New York

[3] a) Ribó JM, Crusats J, Marco M (1994) Tetrahedron **50**: 3967; b) Boiadjiev SE, Anstine DT, Lightner DA (1995) Tetrahedron Asymmetry **6**: 901; c) Crusats J, Farrera JA, Ribó JM (1996) Monatsh Chem **127**: 85

[4] Benitez P, Delgado A, Farrera JA, Ribo JM (1997) Synth Comm **27**: 1697

[5] See *e.g.* Bravo J, Fita I, Gouet P, Jouve HM, Melik-Adamian W, Murshudov GN (1997) Structure of Catalases in Oxidative Stress and the Molecular Biology of Antioxidant Defenses. Cold Spring Harbor Laboratory Press, New York, pp 407–445

[6] Falk H, Schlederer T, Wolschann P (1981) Monatsh Chem **112**: 199

[7] Feliz M, Ribo JM, Salgado A, Trull FR, Vallès MA (1989) Monatsh Chem **120**: 445

[8] Hunter CA, Sanders JKM (1990) J Am Chem Soc **112**: 5525

[9] See (2b), pp 401–422 and the related citations

[10] a) Falk H, Brubmayr K, Neufingerl F (1979) Monatsh Chem **11**: 1127; b) Ausseneg FR, Lippitsch ME, Riegler M (1986) Laser Chem **6**: 269

[11] a) Lehner H, Riemer W, Schaffner K (1979) Liebigs Ann Chem 1798; b) Falk H, Tirring K (1981) Tetrahedron **37**: 761

[12] In linear oligopyrroles it is difficult to distinguish between chiral discrimination induced by a homochiral solvent and the formation of heteroassociates between the oligopyrrole and solvent molecules; a) Braslavsky SE, Holzwarth AR, Langer E, Lehner Matthews I, Schaffner K (1980) Israel J Chem **20**: 196; b) Edinger J, Falk H, Jungwirth W, Müller N, Zruneck U (1986) Monatsh Chem **117**: 849; b) Krois D, Lehner H (1995) Monatsh Chem **126**: 349

[13] a) Haidl E, Krois D, Lehner H (1985) Monatsh Chem **116**: 119; b) Falk H, Kapl G, Medinger W (1985) Monatsh Chem **116**: 1065; c) Haidl E, Krois D, Lehner H (1985) J Chem Soc Perkin Trans 2, 119; d) Krois D, Lehner H (1986) Monatsh Chem **117**: 1205; e) Krois D, Lehner H (1987) J Chem Soc Perkin Trans 2, 219; f) Krois D, Lehner H (1987) J Chem Soc Perkin Trans 2, 1523; g) Krois D, Lehner H (1989) J Chem Soc Perkin Trans 2, 2085; h) Krois D, Lehner H (1990) J Chem Soc Perkin Trans 2, 1745; i) Krois D, Lehner H (1990) J Chem Soc Perkin Trans 2, 1837; j) Krois D (1993) Tetrahedron **49**: 8855

[14] a) Hug W, Wagneire G (1972) Tetrahedron **28**: 1241; b) Blauer G, Wagniere G (1975) J Am Chem Soc **97**: 1949; c) Falk H, Höllbacher G (1978) Monatsh Chem **106**: 97; d) Gaussian 94, Revision B. 3; Frisch MJ, Trucks GW, Schlegel HB, Gill PMW, Johnson BG, Robb MA, Cheeseman JR, Keith T, Petersson GA, Montgomery JA, Raghavachari K, Al-Laham MA, Zakrzewski VG, Ortiz JV, Foresman JB, Peng CY, Ayala PY, Chen W, Wong MW, Andres JL, Replogle ES, Gomperts R, Maartin RL, Fox DJ, Binkley JS, Defrees DJ, Baker J, Steward JP, Head-Gordon M, Gonzalez C, Pople JA (1995) Gaussian, Inc., Pittsburgh, PA
[15] See pp 192–197 of [2b]
[16] a) Günther H (1973) NMR-Spektroskopie. Thieme, Stuttgart, p 173; a) Cookson RC, Crabb TA (1966) Tetrahedron Suppl **7**: 355
[17] Universal Force Field with Charge Equilibration scheme using the interface Cerius 2 (Molecular Simulations); a) Rappe AK, Goddard III WA (1991) J Phys Chem **95**: 3358; b) Rappe AK, Casewit CJ, Colwell KS, Goddard III WA; Skiff WM (1992) J Am Chem Soc **114**: 10024
[18] See for examples p 220 of [2b]
[19] Neuhaus D, Williamson M (1989) The Nuclear Overhauser Effect in Structural and Conformational Analysis. Verlag Chemie, New York, p 95
[20] Janson T, Katz JJ (1972) J Magn Reson **6**: 209
[21] Fita I (private communication)
[22] McDonagh AF, Palma LA (1980) Biochem J **189**: 193
[23] a) Monti D, Manitto P (1981) Synth Comm **11**: 811; b) Ma JS, Lightner DA (1984) J Heterocyclic Chem **21**: 1005; c) Reisinger M, Trull FR, Lightner DA (1985) J Heterocyclic Chem **22**: 1221

Received November 27, 1997. Accepted December 3, 1997